

Simulation of a Polyimide Based Micromirror

A. Arevalo^{*1}, S. Ilyas^{**1}, D. Conchouso and I. G. Foulds^{*1,2}

^{*} Computer, Electrical and Mathematical Sciences and Engineering Division (CEMSE),

^{**} Physical Sciences and Engineering (PSE),

¹King Abdullah University of Science and Technology, Thuwal, Kingdom of Saudi Arabia

²School of Engineering, University of British Columbia - Okanagan, Vancouver, BC, Canada

*Corresponding author: Thuwal 23955-6900, Kingdom of Saudi Arabia, aryps.arevalo@kaust.edu.sa

Abstract: In our work we present the simulation of a micro-mirror using polyimide as the structural material. The simulation was used to verify the initial design parameters and to explore the different characteristics of the electromechanical device. For simulation simplicity the electrodes are integrated as part of the structural layer. The device thickness is 6 μm while the electrodes are 300 nm thick. For the actuation of the device, several configuration of input voltage are simulated to extract the device characteristics. Due to the difference in electrode area size the structure will have a torsion that will deform the cantilever to the larger area electrode side. Using this principle, we could control the tilt of the micro-mirror depending on the input voltage.

Keywords: MEMS, micro-mirror, electrostatic actuator, switch.

1. Introduction

MEMS devices have enabled researchers to provide mechanical solutions for various advanced technologies. In the past two decades polyimide, SU-8 and other polymeric materials have been widely used as a structural material for MEMS devices such as: antennas [1], gyroscopes & accelerometers, sensors & actuators [2], amongst others [3-8]. Mechanical relays have been used to perform digital logic operations instead of transistors [2]. CMOS technology has several challenges, such as its non-zero off state leakage which increases with scaling down of the systems, hence resulting in low energy efficiency [8]. Also in case of the transistor, a variation in temperature causes the semiconductor to return to its intrinsic behavior, which results in an uncontrolled behavior of the device [9]. Furthermore, the CMOS transistors react badly to ionized radiations and hence cannot work in harsh environment conditions [10, 11]. MEMS logic gates zero I_{OFF} and abrupt switching behavior provides a very good

alternative to transistor based logic devices [12]. An electrostatic micromechanical switch for logic operation in multichip modules has previously been proposed on silicon [13]. This was an example of the early designs in MEMS switches. The switch consists of two fixed driving electrodes; two fixed contact electrodes, two movable drive electrodes and one movable contact electrode. A driving voltage is applied to either or both of the fixed drive electrodes. The resulting electrostatic force pulls the movable contact electrode down, and the contacts are put together closing the circuit. By applying this principle and designing specific switch configuration a true mechanical logic gate can be achieved.

3. Device Design and Fabrication

Our micro-mirror is similar to a mechanical relay switch [13]. The design consists of a bridge with two extended wings from the center creating a long pinned cantilever. Figure 1 shows such structure.

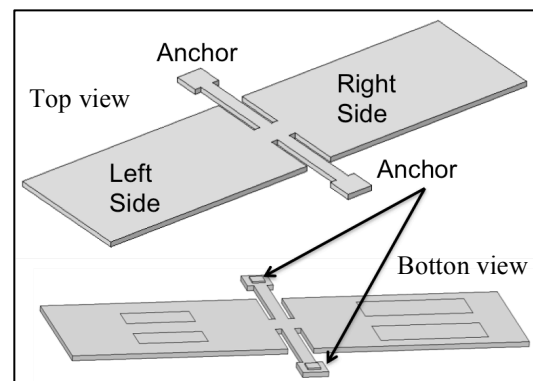


Figure 1. Top and bottom view of the 3D model of the proposed micro-mirror.

Two pairs of electrodes are located on the bottom of the structure in each side of the wing-like plates; two left electrodes (80 μm X 30 μm) and two right electrodes (125 μm X 42.5 μm),

see Figure 2. The micro-mirror and electrodes are initially separated by 2 μm from the substrate. The substrate acts as a common ground for the entire device, while the top electrodes are set to a different potential for the device actuation. The device has an overall size of 535 μm in width, 150 μm in length and a total of 8 μm in height.

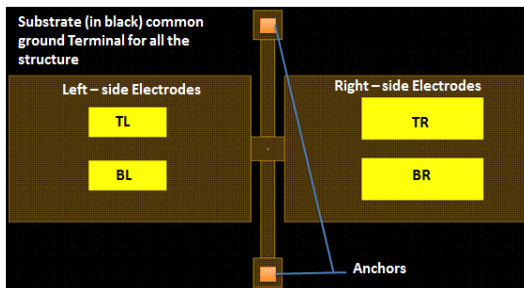


Figure 2. Top layout view of the micro-mirror, emphasizing the location of the top electrodes.

The electrodes can be in two different states: active (when a voltage different than 0 Volts applied to the electrode) and inactive (when no voltage is applied to the electrode). The different configurations of interest for us are:

1. When TR (Top Right) and BR (Bottom Right) electrodes are active and the other two are inactive.
2. When TR (Top Right) and BL (Bottom Left) electrodes are active and the other two are inactive.
3. When TL (Top Left) and BL (Bottom Left) electrodes are active and the other two are inactive.

The devices are fabricated using our In-House process based on polyimide as the structural material and three different metal layers that can be interconnected. Figure 3 shows an SEM (Scanning Electron Microscope) image of a fabricated device. The first metal layer is deposited on a silicon wafer as bilayer metal of chromium and gold with a total thickness of 300nm. The second metal layer is attached and patterned under the structure to create the different electrodes. The structural layer is polyimide and has a nominal thickness value of 6 μm. A third metal layer is deposited on the top of the structural layer to overcome any bimorph

bending effect due to the difference of stresses between the layers.

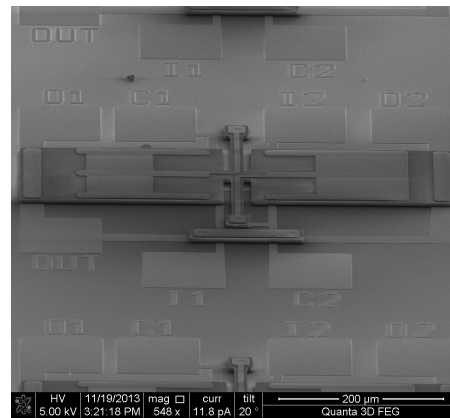


Figure 3. SEM image of fabricated micro-mirror.

A basic set of equations for the electrostatic and mechanical torsion were used to get initial understanding of the working dimensions of the proposed design. The operating voltage was fixed in the range of 0 – 15 Volts, to perform an initial analysis to get the devices characteristics. The force on the beam due to electrostatic attraction between the ground electrode and the top electrode can be approximated or simplified to the case of two parallel plates. The attraction force can be calculated by using the formula for electrostatic attraction between parallel plates:

$$F = \frac{\epsilon AV^2}{2d^2} \dots\dots\dots(1)$$

Where:
 F = Attraction force
 A = Plate Area
 V = Applied Voltage
 d = Gap between plates
 ε = Permittivity

The force acts on the plate as a distributed force but it can be modeled as a single force acting on one point. By multiplying this force times the distance to the axis of rotation, we can calculate the torque produced by the particular electrode.

$$T = r \times F \dots\dots\dots(2)$$

Where:
 r = Arm moment of the force

As described previously the proposed structure has two long cantilevers that extend from the anchored central bridge. These cantilevers will be exposed to the electrostatic forces, which in turn will cause them to bend and to contact the substrate on the desired side of the structure. The torsion of similar structures to these cantilevers has been previously studied and it can be expressed by [15]:

$$K_t = \frac{1}{3L} Gwh^3 \cdot \left(1 - 0.6324 \frac{h}{w}\right) \dots \dots \dots (3)$$

Where:

K_t = Torsional Stiffness

G = Shear modulus

h = Height of the cantilever

w = Width of the cantilever

In COMSOL, the electrostatic field in the air and in the beam is governed by Poisson's equation:

$$-\nabla \cdot (\epsilon \nabla V) = 0 \dots \dots \dots (4)$$

Where the derivatives are used with respect to the spatial coordinates. The numerical model represents the electric potential and its derivatives on a mesh, which are changing with respect to the spatial frame. The structure is supplied with a voltage terminal with a specific bias potential, V_0 . The bottom of the model is grounded, and the rest of the boundaries are electrically insulated. The terminal boundary condition can automatically compute the capacitance of the system. The force density that acts on the wings like cantilever beams results from Maxwell's stress tensor:

$$F_{es} = -\frac{1}{2} (E \cdot D)n + (n \cdot E)D \dots \dots \dots (4)$$

Where:

E = Electric Field Vector

D = Electric Displacement Vector

n = Outward Normal Vector of the Boundary.

4. Simulation Results

Simulations had an affirmative response between the deformation of the cantilever beam and the electrostatic forces. The generated forces

bend the cantilever and due to this deformation the gap between the electrodes is reduced. The closer the electrodes are, the greater the attraction forces that they experienced. When the electrostatic forces overcome the stress forces the system becomes unstable, and the gap between the electrodes collapses. The voltage needed to collapse the structure is also called the pull-in voltage. When the applied voltage is lower than the pull-in voltage, the structure stays at equilibrium, where the stress forces are in balance with the electrostatic forces. Figure 4 shows the simulation results of an applied voltage, which is lower than the pull-in voltage and the corresponding displacement of the structure.

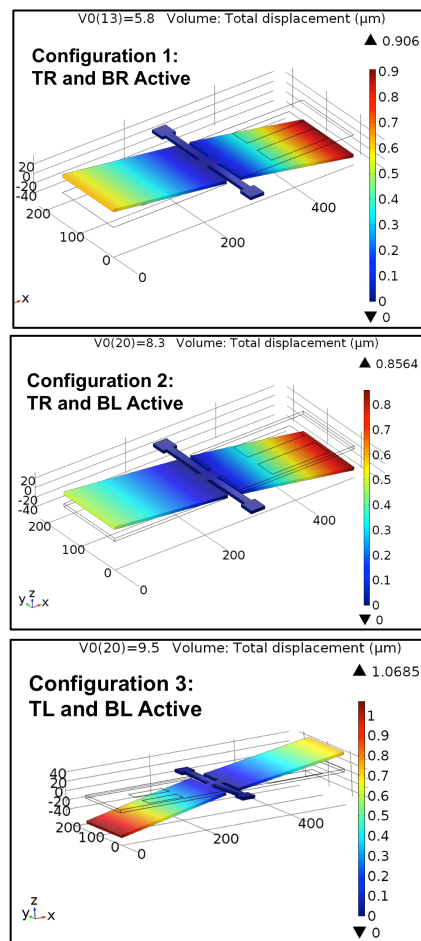


Figure 4. Micro-mirror simulation for the different active electrodes configuration, showing the displacement at a lower voltage than the pull-in voltage. The deformation is exaggerated by 50 times for visualization purposes and displacement is not greater than the gap between the electrodes.

In Figure 5, the shape of the cantilever's deflection is presented for each applied voltage. This study was done by plotting the z-displacement of a 3D Cut Line defined in the middle and across the length of the structure.

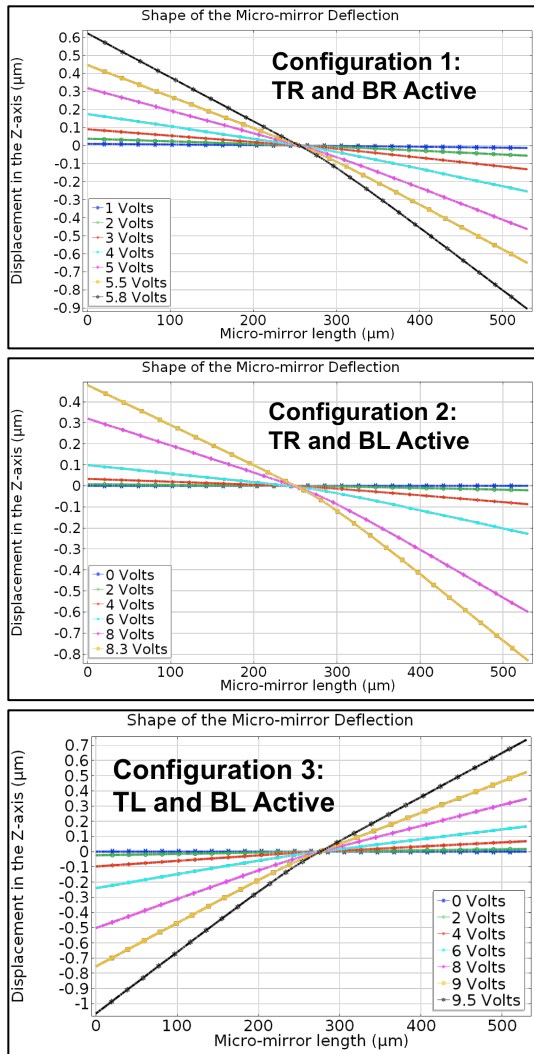


Figure 5. Shape of the Micro-mirror deflection for different applied voltages and different active electrodes configuration.

The deflection at the tip is plotted in Figure 6 as a function of applied voltage. It has to be noted that by applying higher voltages than the pull-in voltage, the solution will not converge for a Stationary Study, as there will not be a stable stationary solution. In our case, we are interested in the three different modes of operation previously described, which gives us three

different pull-in voltages depending on the electrodes that are active.

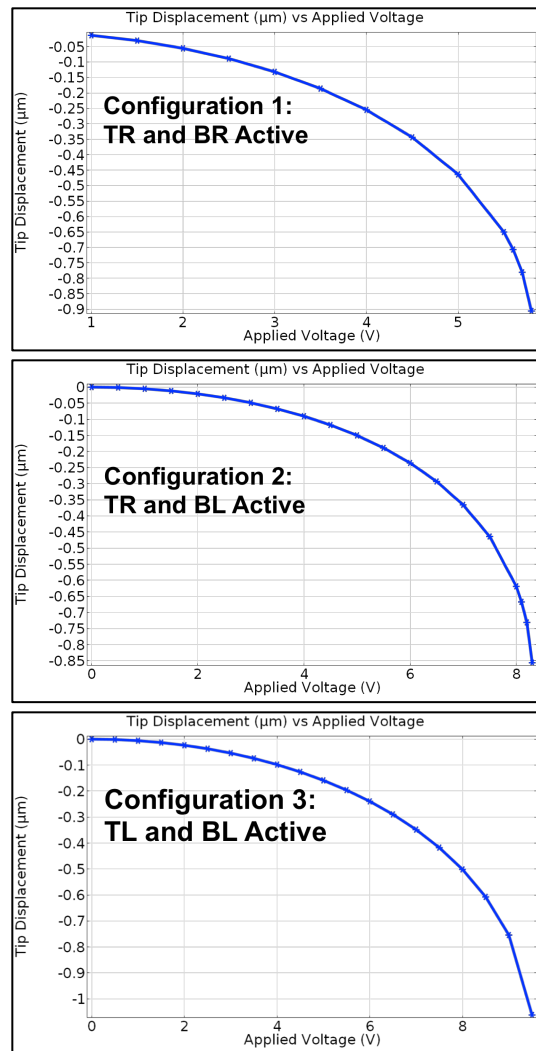


Figure 6. Tip displacement against the different applied voltages for the 9.5.

Figure 7 shows the DC Capacitance – Voltage curves that are predicted for the micro-mirror structure for the three different cases. The simulation is consistent to that of the behavior of an ideal parallel plate capacitor. In such ideal configuration, the capacitance increases with the decrease in distance between the plates. Nevertheless, the effect does not account for all the change in capacitance observed and most of it is due to the gradual softening of the coupled electromechanical system. This indicates a larger structural response for a given voltage increment

at higher bias. Therefore, more charge needs to be added to retain the voltage difference between the electrodes.

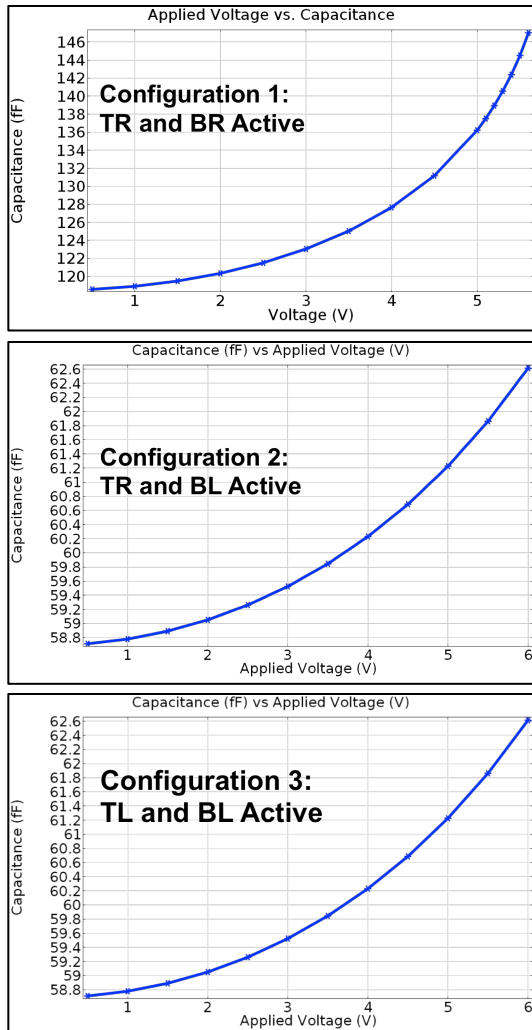


Figure 7. Micro-mirror tip displacement vs. capacitance plot for the different active electrode configuration.

5. Conclusions

In this work we have presented a simulation characterization of the proposed micro-mirror design. Simulation results showed that there are, three different operating voltages and each causes the device to pull-in to one or the other side depending on the design parameters like electrode dimension. This feature of the micro-mirror opens up prospects for using such structure as a switch to realize various kinds of

logic operations such as AND, NAND, Inverter, etc. The conceptual model was fabricated with our In-House Multiuser fabrication process. Future work will be focused on further improving the design to implement various logic operations using same structure and principle of operation.

6. References

1. L. Marnat, A. Arevalo et al., "New Movable Plate for Efficient Millimeter Wave Vertical on-Chip Antenna," *IEEE Transactions on Antennas and Propagation*, vol. 61, pp. 1608-1615. (2013)
2. Lee S W et al., MEMS mechanical logic units: design and fabrication with micragem and polymumps, *Proc. Canadian Conf. on Electrical and Computer Engineering (Saskatoon, Canada, 1-4 May 2005)* pp 1513-6. (2005)
3. Alfadhel, A, A. Arevalo et al., "Three-Axis Magnetic Field Induction Sensor Realized on Buckled Cantilever Plate," *Magnetics, IEEE Transactions on*, vol.49, no.7, pp. 4144, 4147. (2013).
4. A. Arevalo and Ian G. Foulds, "Parametric Study of Polyimide-Lead Zirconate Titanate Thin Film Cantilevers for Transducer Applications", 2013 COMSOL Conference, Rotterdam, Holland. (2013)
5. A. A. Arévalo Carreño et al., "Simulation of a Low Frequency Z-axis SU-8 Accelerometer in CoventorWare and MEMS+", *UKSIM2013*. 6.
6. D. Conchouso, A. A. Arévalo Carreño et al., "Simulation of SU-8 Frequency-Driven Scratch Drive Actuators", *UKSIM2013*. (2013)
7. A. A. A. Carreno et al., "Optimized Cantilever-to-Anchor Configurations of Buckled Cantilever Plate Structures for Transducer Applications", *COMSOL Conference, Milan, Italy*. (2012)
7. A. A. A. Carreno et al., "UHeater on a Buckled Cantilever Plate for Gas Sensor Applications", *COMSOL Conference, Milan, Italy*. (2012)
8. S. Hanson, B. Zhai, K. Bernstein, D. Blaauw, A. Bryant, L. Chang, K. K. Das, W. Haensch, E. J. Nowak, and D. M. Sylvester, "Ultralowvoltage, minimum-energy CMOS," *IBM J. Res. & Dev.*, vol. 50, no. 4/5, pp. 469-490. (2006)
9. B Streetman and S Banerjee, "Solid State Electronic Devices", Prentice Hall, New Jersey. (1999)

10. J R Srour and J M McGarrity, "Radiation Effects on Microelectronics in Space" Proceedings of the IEEE, Vol. 76, No. 11. (1988)
11. R W Johnstone et al., "The effects of proton irradiation on electrothermal micro-actuators," Canadian Journal of Electrical and Computer Engineering, Vol. 27, No. 1, pp. 3-5. (2002)
12. F. Chen et al., "Integrated circuit design with NEM relays," in Proc. IEEE/ACM Int'l Conf. Comput.-Aided Des., pp. 750- 757. (2008)
13. Hirata A. et al., "A electrostatic micromechanical switch for logic operation in multichip modules on Si Sensors Actuators" A 80 119-25. (2000)
14. J. Jeon et al., "Seesaw Relay Logic and Memory Circuits," IEEE/ASME J.Micromech. Syst. Lett., vol. 31, no. 4, pp. 1012-1014. (2010)
15. C.-Y. Tsai, T.-L. Chen, "Design, fabrication and calibration of MEMS logic gate," J. Micromech. Microeng. 11pp. (2010)
16. R. Nathanael et al., "4-terminal relay technology for complementary logic," in IEEE IEDM Tech. Dig., , pp. 223-226. (2009)
17. R. Parsa et al., "Nanoelectromechanical relays with decoupled electrode and suspension," in IEEE MEMS Cancun, Mexico. (2011)
18. N. Sinha, T. S. Jones, G. Zhijun, and G. Piazza, "Body-biased complementary logic implemented using AlN piezoelectric MEMS switches," in Electron Devices Meeting (IEDM), 2009 IEEE International, pp. 1-4. (2009)